PHILOSOPHICAL TRANSACTIONS OF THE ROYAL SOCIETY A

Phil. Trans. R. Soc. A (2008) **366**, 3503–3523
doi:10.1098/rsta.2008.0110
Published online 16 July 2008

Cell coupling in mouse pancreatic β-cells measured in intact islets of Langerhans

By Quan Zhang[1], Juris Galvanovskis[1], Fernando Abdulkader[1,2], Christopher J. Partridge[1], Sven O. Göpel[4], Lena Eliasson[3,*] and Patrik Rorsman[1]

[1]*Oxford Centre for Diabetes, Endocrinology and Metabolism, University of Oxford, Churchill Hospital, Oxford OX3 7LJ, UK*
[2]*Department of Physiology and Biophysics, Institute of Biomedical Sciences, University of São Paulo, 05508-900 São Paulo, Brazil*
[3]*Lund University Diabetes Centre, Clinical Research Center, 205 02 Malmö, Sweden*
[4]*AstraZeneca R&D, Pepparedsleden 1, 43183 Mölndal, Sweden*

The perforated whole-cell configuration of the patch-clamp technique was applied to functionally identified β-cells in intact mouse pancreatic islets to study the extent of cell coupling between adjacent β-cells. Using a combination of current- and voltage-clamp recordings, the *total* gap junctional conductance between β-cells in an islet was estimated to be 1.22 nS. The analysis of the current waveforms in a voltage-clamped cell (due to the firing of an action potential in a neighbouring cell) suggested that the gap junctional conductance between a pair of β-cells was 0.17 nS. Subthreshold voltage-clamp depolarization (to −55 mV) gave rise to a slow capacitive current indicative of coupling between β-cells, but not in non-β-cells, with a time constant of 13.5 ms and a total charge movement of 0.2 pC. Our data suggest that a superficial β-cell in an islet is in electrical contact with six to seven other β-cells. No evidence for dye coupling was obtained when cells were dialysed with Lucifer yellow even when electrical coupling was apparent. The correction of the measured resting conductance for the contribution of the gap junctional conductance indicated that the whole-cell K_{ATP} channel conductance ($G_{K,ATP}$) falls from approximately 2.5 nS in the absence of glucose to 0.1 nS at 15 mM glucose with an estimated IC_{50} of approximately 4 mM. Theoretical considerations indicate that the coupling between β-cells within the islet is sufficient to allow propagation of $[Ca^{2+}]_i$ waves to spread with a speed of approximately 80 μm s^{-1}, similar to that observed experimentally in confocal $[Ca^{2+}]_i$ imaging.

Keywords: β-cell; pancreatic islets; cell coupling; gap junctions; K_{ATP} channels

1. Introduction

The pancreatic islet is a complex organ consisting of approximately 1000 cells of which the insulin-producing β-cells comprise 70–80 per cent in mice (Pipeleers 1987). Islet cells are electrically excitable and use electrical signals to couple

* Author for correspondence (lena.eliasson@med.lu.se).

One contribution of 12 to a Theme Issue 'Biomedical applications of systems biology and biological physics'.

changes in blood glucose concentration to stimulation or inhibition of hormone release (Henquin & Meissner 1984; Ashcroft & Rorsman 1989). The application of the patch-clamp technique to pancreatic islet cells has revolutionized our concepts about the stimulus–secretion coupling of the insulin-producing β-cells (Ashcroft & Rorsman 1989). These studies have revealed that ATP-regulated K^+ channels (K_{ATP} channels) play a central role in linking changes in plasma glucose concentration to stimulation or inhibition of insulin secretion. The K_{ATP} channels are active in the absence of glucose (when the cytoplasmic ATP/ADP ratio is low). An increase in glucose leads, via a metabolically induced increase in the ATP/ADP ratio, to the closure of the K_{ATP} channels, which results in membrane depolarization, action potential firing, opening of voltage-gated Ca^{2+} channels, an increase in cytoplasmic $[Ca^{2+}]_i$ and the initiation of exocytosis of insulin-containing secretory granules (Rorsman & Renström 2003). To date, almost all patch-clamp studies on β-cells have been carried out on isolated islet cells maintained in short-term tissue culture. Accumulating evidence indicates that the cellular properties may change during culture in an artificial medium containing foetal calf serum and when the cells are deprived of their normal environment (Göpel *et al.* 1999*b*). We have developed methods that allow patch-clamp measurements to be applied to islet cells within the intact islet (Göpel *et al.* 1999*a*,*b*, 2000*a*,*b*; Kanno *et al.* 2002). These studies have revealed that the electrophysiological properties of β-cells within the intact islet differ from those of isolated cells in several respects such as channel density and voltage dependence of their activation and inactivation, etc.

In the intact pancreatic islets, intercellular signalling can occur via both chemical (paracrine; Rorsman *et al.* 1989; Salehi *et al.* 2005) and electrical (via gap junctions; Charollais *et al.* 2000) signals. Both pathways of communication are disrupted when the islet is dissociated into single cells as is traditionally done prior to patch-clamp characterization. The functional significance of intercellular signalling is suggested by the fact that isolated β-cells exhibit a much poorer secretory capacity than β-cells in the intact islet (Pipeleers *et al.* 1982; Luther *et al.* 2006).

Evidence for electrical coupling via gap junctions between islet cells has previously been provided by electron microscopy (Orci *et al.* 1975), recordings of membrane potential and currents using sharp intracellular electrodes (Meissner 1976; Eddlestone *et al.* 1984; Mears *et al.* 1995), patch-clamp experiments on isolated islet cell pairs (Perez-Armendariz *et al.* 1991) and dye coupling (Michaels & Sheridan 1981; Charollais *et al.* 2000). It has in fact been proposed that the β-cells function as a 'secretory syncytium' (Santos *et al.* 1991). Gap junctions are formed by a family of proteins called connexins (Willecke *et al.* 2002). The most recent evidence has suggested that islet cells express connexin-36 (Calabrese *et al.* 2003). The gap junctions probably serve to synchronize electrical activity and secretion in β-cells in different parts of pancreatic islets (Eddlestone *et al.* 1984; Santos *et al.* 1991). However, it is less clear whether β-cells are also in electrical contact with neighbouring non-β-cells. Evidence for heterologous coupling was originally provided by dye-injection experiments (Michaels & Sheridan 1981; Meda *et al.* 1986), but functional studies (Göpel *et al.* 1999*a*; Nadal *et al.* 1999) suggest that coupling between β-cells and non-β-cells is weak.

Here, we have analysed the coupling between β-cells in intact islets using the whole-islet patch-clamp approach (Göpel *et al.* 1999*a*). We found that the gap junctional conductance between pairs of β-cells is approximately 0.17 nS and that each β-cell on average makes contact with another seven β-cells.

2. Materials and methods

(*a*) *Islet preparation*

Pancreatic islets were isolated from Naval Medical Research Institute mice. The mice were killed by cervical dislocation. Islets were obtained by collagenase digestion and maintained in short-term (6–24 hours) tissue culture as described elsewhere (Göpel *et al.* 1999*a*,*b*).

(*b*) *Solutions*

The standard extracellular solution was used for the recordings from intact islets, which consisted of (in mM) 140 NaCl, 3.6 KCl, 2 $NaHCO_3$, 0.5 NaH_2PO_4, 0.5 $MgSO_4$, 2.5 $CaCl_2$, 5 HEPES (pH 7.4, adjusted with NaOH) and (unless otherwise indicated) 5 glucose. To block voltage-activated outward delayed rectifying K^+ currents, 20 mM tetraethylammonium chloride (TEACl) was included in the extracellular medium in all experiments unless otherwise indicated. When TEA was present in the solution, the concentration of NaCl was correspondingly reduced to maintain iso-osmolarity. The pipette solution used consisted of (in mM) 76 K_2SO_4, 10 NaCl, 10 KCl, 1 $MgCl_2$ and 5 HEPES (pH 7.35 with KOH).The perfusion solution used in Ca^{2+} imaging in intact islets contained (in mM) 140 NaCl, 3.6 KCl, 2 $NaHCO_3$, 0.5 NaH_2PO_4, 0.5 $MgSO_4$, 2.5 $CaCl_2$, 5 HEPES (pH was adjusted to 7.4 with NaOH) and 1 or 20 glucose.

(*c*) *Electrophysiology*

All electrophysiological measurements except those in figure 4 were performed using the perforated patch whole-cell technique using an EPC-9 patch amplifier controlled by the software package Pulse (Heka Electronics, Lambrecht, Germany; see details in Göpel *et al.* 1999*a*). Pancreatic β-cells were identified by the absence of voltage-gated Na^+ currents when holding at −70 mV and the generation of oscillatory electrical activity when exposed to 10–15 mM glucose as described elsewhere (Göpel *et al.* 1999*a*). Non-β-cells were identified by the presence of a prominent voltage-gated Na^+ current that remained observable when holding at −70 mV (Göpel *et al.* 1999*a*). All electrophysiological experiments were carried out at 32°C. The use of a subphysiological temperature improves membrane stability and thereby facilitates the electrophysiological measurements while maintaining secretory function (Renström *et al.* 1996).

(*d*) *Ca^{2+} imaging*

Intact islets were loaded in standard RPMI1640 tissue culture medium with the membrane-permeable Ca^{2+} dye fluo-4AM (1 μM; from Invitrogen) in the presence of 0.01 per cent pluronic acid for 30 min at 37°C. For these experiments, the islets were fixed with a wide-bore holding pipette within a continuously

superfused and temperature-controlled (37°C) bath on an Axioskop 2 FS-mot microscope (Carl Zeiss, Jena, Germany; http://www.zeiss.com). Laser scanning confocal microscopy was performed using an LSM 510 META laser scanning module (Carl Zeiss, Jena, Germany). The Ca^{2+} indicator was excited with a 488 nm argon laser, and emitted fluorescent light was collected through a 500–550 nm band-pass filter. Increases in intracellular Ca^{2+} are displayed as upward deflections. Images were acquired at 393 ms intervals. The recordings were replayed off-line and regions of interest were selected and analysed using the Zeiss LSM 510 software.

(*e*) *Dye coupling*

The intracellular medium was supplemented with 2 μM of Lucifer yellow (Li^+ salt; Invitrogen). Lucifer yellow was loaded into the cell via a patch-clamp electrode (during standard whole-cell recordings), filled with an intracellular medium containing (in mM) 125 CsCl, 10 NaCl, 1 $MgCl_2$, 0.05 EGTA, 3 Mg-ATP, 0.1 cAMP and 5 HEPES (pH 7.1 using CsOH). The spread of Lucifer yellow fluorescence was monitored using a Bio-Rad Radiance 2100 confocal system (Carl Zeiss CellScience Ltd, Jena, Germany) using the 457 nm line of an argon laser. The emission of the dye was detected above 500 nm.

(*f*) *Data analysis*

All data are presented as mean values ± s.e.m. of indicated number of cells. Statistical significances were evaluated with Student's *t*-test.

3. Results

(*a*) *Evidence for electrical coupling between β-cells in intact islets*

Figure 1*a*(i) shows a membrane potential recorded from a β-cell within an intact islet exposed to 10 mM glucose using the perforated patch whole-cell technique. Membrane potential oscillated between a depolarized plateau with action potentials superimposed on it, and repolarized electrically silent periods. This type of electrical activity is regarded as a hallmark of the β-cell (Henquin & Meissner 1984) and is traditionally used for the functional identification of the β-cells. In a series of 20 experiments, the most negative voltage between the burst of action potentials and the plateau potential averaged $V_i = -55 \pm 2$ mV and $V_p = -40 \pm 1$ mV, respectively.

The amplifier was then switched into the voltage-clamp mode and the membrane potential was held at −70 mV. Under these conditions, the holding current recorded in the same cell as that used for the membrane potential recordings oscillated spontaneously and waveforms reminiscent of upside down bursts of action potentials were seen (figure 1*a*(ii)). These current oscillations are attributable to bursts of action potentials in the neighbouring unclamped cell(s) (Mears *et al.* 1995; Göpel *et al.* 1999*a*). In a series of 20 experiments, the holding current oscillated between a level of $I_i = -18 \pm 3$ pA during the silent period and $I_p = -35 \pm 4$ pA during the plateau phase. The measurements reported here were made using voltage and current records containing several bursts and thus represent the average of these parameters in the individual cell.

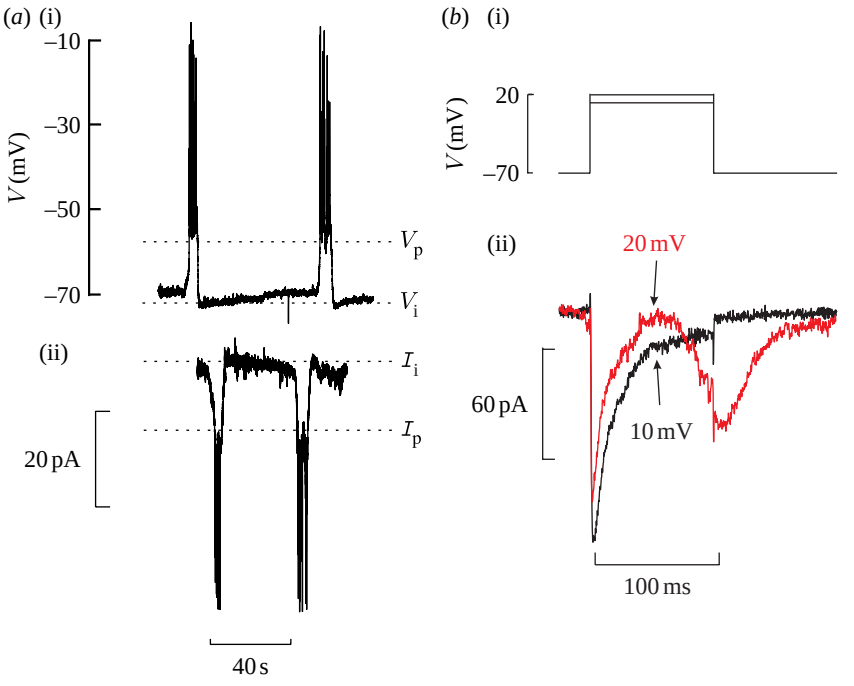

Figure 1. Cell coupling between β-cells in intact pancreatic islets. (*a*(i)) Membrane potential recording and (ii) oscillating holding current recorded from the same cell after switching from current-clamp into voltage-clamp mode. The islet was exposed to 10 mM glucose. The dotted horizontal lines indicate the plateau potential (V_p), the most negative voltage attained following the termination of a burst and depolarization (V_i), the holding current in the electrically silent cell (I_i) and the plateau current from which the 'action currents' originate (I_p). (*b*) Whole-cell currents recorded from β-cells in an intact islet during voltage-clamp depolarizations from −70 mV to +10 (black trace) or +20 mV (red trace). Note that whereas voltage-clamp depolarization to +10 mV elicits only an inactivating Ca^{2+} current, the current response evoked by the pulse to +20 mV is contaminated with an action current that reflects an action potential generated in one of the electrically coupled neighbours.

We used the plateau and interburst voltages and currents rather than the action potentials for these calculations as the latter are highly variable and would result in large errors. We and others have previously reported that the gap junctional conductance only changes marginally (approx. 10%, if at all) during the active and silent phases (Mears *et al.* 1995; Göpel *et al.* 1999*b*; but see Andreu *et al.* 1997). Assuming that the membrane potential in the neighbouring cells oscillates in the same way as it does in the cell in direct contact with the patch electrode, the gap junctional conductance ($G_{j,tot}$) can be calculated using the relationship (Mears *et al.* 1995)

$$G_{j,tot} = (I_i - I_p)/(V_p - V_i). \tag{3.1}$$

We thus derived an average value of $G_{j,tot}$ of 1.22 ± 0.16 nS ($n=20$) for the *total* conductance due to cell coupling. The observed current deflections represent the sum of currents injected from *all* neighbouring cells.

(*b*) *Electrical coupling between individual pairs of β-cells*

As previously reported, voltage-clamp currents can be recorded from β-cells in intact islets (Göpel *et al.* 1999*a*, 2000*a*). An example of a perforated patch whole-cell Ca^{2+} current recording from a β-cell in an intact islet is shown figure 1*b*. Under these experimental conditions (TEA present in the extracellular medium), the depolarization of the cell membrane to potentials below +10 mV elicited pure voltage-clamp currents (after the removal of linear capacitive and resistive components), i.e. currents flowing through the ion channels localized in the plasma membrane of the cell connected to the recording electrode (figure 1*b*, black curve in (ii)). However, depolarization of the cell to more positive voltages occasionally caused secondary current waveforms that were superimposed on the voltage-clamp Ca^{2+} currents recorded (figure 1*b*, red curve in (ii)). By analogy to what has been described in chromaffin cells (Moser 1998), we attribute these secondary waveforms to the firing of an action potential in neighbouring cells. During the depolarization of the voltage-clamped cell, current spread into the electrically coupled neighbours results in the concurrent depolarization of these cells. As the stimulus is increased, the threshold for firing of an action potential is approached and eventually exceeded. Assuming that the neighbours are not perfectly synchronized or equally connected, the current waveform can be used to estimate the conductance between the voltage-clamped cell and its *best* coupled neighbour. In a series of seven experiments, secondary action potential waveforms were first observed when the patch-clamped cell was depolarized from −70 mV to an average of 16±4 mV. Thus, the voltage-clamped cell must be depolarized by 86 mV with respect to the holding potential (−70 mV) to elicit an action potential in at least one of its neighbours.

How much of this voltage change is actually sensed by the neighbour? To answer this question, we recorded action potentials from a β-cell in an islet exposed to 10 mM glucose before and after the addition of 20 mM of TEACl (figure 2*a*), the broad-spectrum blocker of (voltage-gated) K^+ channels (Hille 2001). Consistent with earlier reports (Atwater *et al.* 1979), addition of TEA^+ converts the normal oscillatory glucose-induced electrical activity to continuous firing of large overshooting action potentials starting from a fairly repolarized membrane potential. We determined the threshold for action potential firing in the presence of TEA. The threshold was defined as the voltage at which the rapid upstroke of the action potential commenced. In a series of nine experiments, the threshold potential averaged −48±1 mV.

We also determined the threshold when the recordings were made in the presence of 5 mM glucose and 20 mM TEA when the cell was stimulated by depolarizing current pulses, i.e. the conditions used for the voltage-clamp measurements presented in figure 1*b*. A recording from a cell in which injection of 10 pA was required to evoke an action potential (grey curve) is shown in figure 2*b*. The corresponding threshold potential was approximately −40 mV (figure 2*b*). In a series of six experiments, the first action potential was observed 164±49 ms after the onset of the pulse, which required 18±11 pA of injected current and originated from a threshold potential of −43±2 mV. The latter value should be compared with the membrane potential of the β-cell in the presence of 5 mM glucose and 20 mM TEA, which amounted to −70±2 mV (n=16). Thus, the membrane of the neighbouring cell in figure 1*b* must depolarize by 27 mV, from −70 mV to −43 mV to attain the threshold for action potential firing.

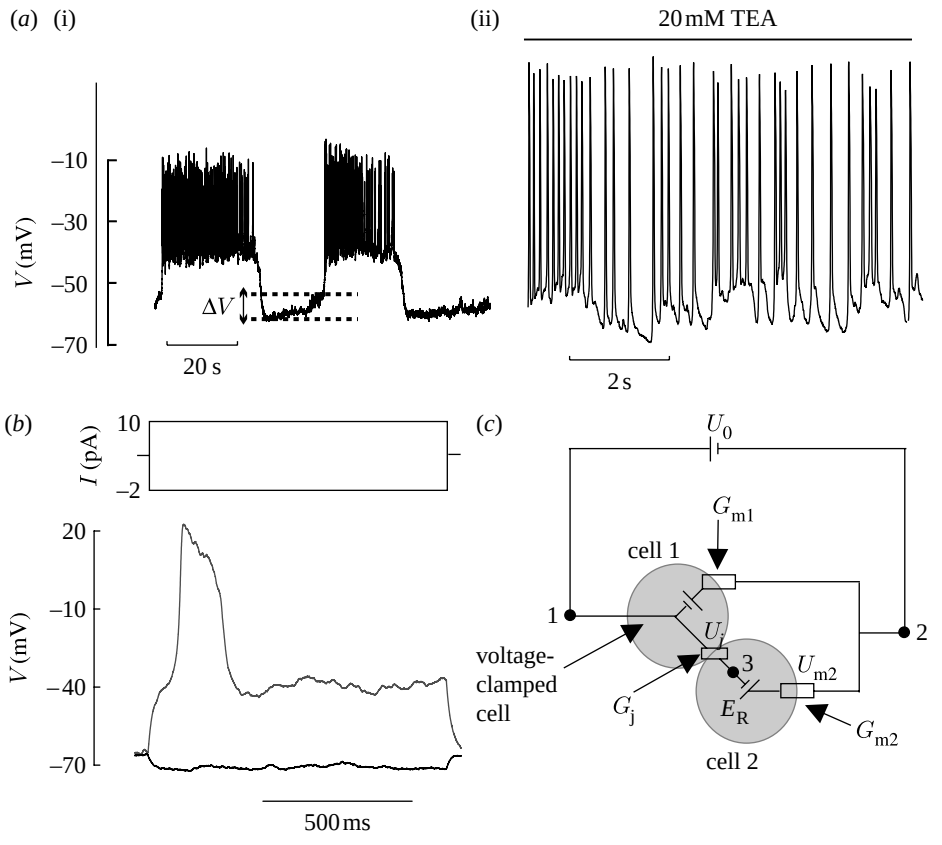

Figure 2. Threshold for action potential firing in β-cells. (*a*) Electrical activity recorded in the presence of 10 mM glucose (i) before and (ii) after the inclusion of 20 mM of TEA. The definition of ΔV is indicated by the dotted lines and the arrow. (*b*) Membrane potential responses were obtained by injecting 2 pA and +10 pA of current into the cell via the patch electrode. The large waveform (grey curve) superimposed on the passive response (black curve) reflects an action potential with a threshold of approximately −40 mV. (*c*) Equivalent electrical circuit of two coupled cells within an islet. Cell 1 is connected to the patch electrode and voltage clamped. A current in cell 1 can exit either via the plasma membrane (G_{m1}) or through the gap junction into cell 2 (G_j). Note that G_{m1} and ($G_c + G_{m2}$) are coupled in parallel and that the voltage clamp of cell 1 accordingly is unperturbed by electrical coupling. Cell 2 contains an electromotive force represented by the element E_R and which corresponds to the membrane potential of cell 2 (−68 mV).

(*c*) *Equivalent circuit of two electrically coupled β-cells*

An equivalent electric circuit of the voltage-clamped cell (cell 1) and one of its closest electrically coupled neighbours (cell 2) is shown in figure 2*c*. Here, the membrane conductance of the first cell (G_{m1}) and the coupling conductance (G_j) between the two cells are connected in parallel as will be the coupling conductance of any other cell joined directly to cell 1. Accordingly, the coupling of cells in an islet does not interfere with the clamping of the membrane potential in cell 1. The circuit may seem overly simplistic in considering two coupled cells only, but the inclusion of additional cells joined directly to cell 1 (while increasing the total conductance of gap junctions) neither affects the potential difference across the

gap junctions nor the current flowing between any pair of cells. The influence on cell 1 of cells coupled with it via other cells is assumed to be negligible (Goforth *et al.* 2002).

To estimate the potential difference U_j across the gap junction (figure 2*c*) under conditions that lead to the occurrence of a secondary spike, we made the following considerations. First, as shown above, the spikes occur upon depolarization of cell 1 up to +16 mV. Second, current injection experiments revealed that the threshold for firing an action potential in a β-cell within an intact islet was −43 mV. In terms of the equivalent circuit in figure 2*c*, a secondary current spike in cell 1 will result if the following two conditions are satisfied:

(i) $U(1)-U(2)=16$ mV and
(ii) $U(3)-U(2)=-43$ mV.

Here $U(1)$, $U(2)$ and $U(3)$ are the potentials at the corresponding points of the equivalent circuit (figure 2*c*). Combining these two conditions yields the potential difference across the gap junction,

$$U_j = U(1)-U(3) = 59\ \text{mV}.$$

The conductance of a single gap junction connecting two β-cells can then be estimated by noticing that the voltage drop across the gap junction (U_j) relates to the voltage drop across the membrane of cell 2 (U_{m2}) as the resistance of the gap junction (R_j) relates to the resistance of the membrane of cell 2 (R_{m2}); thus,

$$R_j = \frac{U_j R_{m2}}{U_{m2}}, \tag{3.2}$$

where R_{m2} is the pure input resistance of the membrane with no connections to other cells. We estimated R_{m2} by measuring the input resistance of isolated β-cells exposed to 5 mM glucose and 20 mM TEA, i.e. the same conditions as were used for the measurements of the other parameters of the equivalent circuit (figure 2*c*). In a series of six experiments, R_{m2} was determined to be 2.70 ± 1.7 GΩ. Inserting this value into the above equation and taking into account that the average $U_{m2}=27$ mV (calculated on the basis of the equivalent circuit of coupled cells shown in figure 2*c*) yields a conductance for the gap junction between two adjacent β-cells of 0.17 nS. Comparing this value with the total gap junctional conductance estimated earlier (1.22 nS) suggests that each β-cell is connected to seven other cells (1.22 nS/0.17 nS). It should be noted that this estimate is based on the firing of an action potential in the best coupled neighbour. Thus, the estimate of the number of electrically coupled cells should be regarded as a lower estimate. The estimate also assumes that TEA does not affect the gap junctional conductance. We acknowledge that TEA has been reported to increase the number of gap junctions in rat β-cells by approximately 15 per cent over 90 min (Sheppard & Meda 1981). It is unlikely that this will occur during the short duration of our experiments (a few minutes) and even if it does such an effect will only have a marginal effect on the above estimate of the number of coupled cells.

(*d*) *Analysis of capacitive currents in islets*

An alternative way to detect and evaluate the coupling of cells in islets is the analysis of the transient capacitive currents that are elicited by applying a square voltage stimulus to a patch-clamped cell. As discussed elsewhere (Moser 1998), the transient capacitive current of an isolated cell should consist only of a single rapid component (reflecting the redistribution of charge during the depolarization) that relaxes within less than 1 ms. Usually, this current is cancelled out by the capacitance compensation network of the patch-clamp amplifier (EPC-9, Heka Electronics, Germany). In the presence of electrical coupling, however, the transient capacitive current should consist of at least two components with widely different kinetics: a fast component caused by the recharging of the membrane of the patched cell and a slow component resulting from the charging of the membranes of cells coupled to it. Records of membrane currents obtained using the perforated patch whole-cell technique and evoked by 15 mV depolarizing pulses applied from a holding potential of −70 mV are displayed in figure 3*a*. Although the fast current component in these recordings was almost completely neutralized by the capacitance compensation network of the patch amplifier, an additional slow component of capacitive current remained in β-cells *in situ* (figure 3*a*). This slow current component decayed with a mean time constant of 13.5 ± 1.6 ms ($n=5$). When the same protocol was applied to a single isolated β-cell, the current response quickly settled at a new steady-state level with no sign of a slow uncompensated component (not shown). Moreover, no evidence for the slow component of capacitive current was observed in non-β-cells. The remaining rapid transients remaining in the non-β-cells we attribute to imperfect compensation of the pipette capacitance.

The capacitance C_{m} that represents all cells coupled to the patch-clamped cell is charged via the gap junctions with conductance $G_{\mathrm{j,tot}}$. The time constant of this process is dependent on $G_{\mathrm{j,tot}}$ (or $R_{\mathrm{j,tot}}$) and the total capacitance C_{m} and conductance G_{m} (or resistance, R_{m}) of the membranes of coupled cells. The set of resistances and capacitances of n identical coupled cells is represented by an equivalent circuit shown in figure 3*b*. This circuit consists of n branches connected in parallel and made of the resistance of the gap junction from the patched cell R_{j} (G_{j}) to the coupled neighbour as well as the neighbour's membrane resistance R_{m1} (G_{m1}) and membrane capacitance C_{m1}. If we assume that all β-cells within an islet are electrically identical, we can substitute this circuit with the simpler circuit shown in figure 3*c*.

The simplified circuit is made up of a resistance $R_{\mathrm{j,tot}}$ ($G_{\mathrm{j,tot}}$), corresponding to the total resistance of all gap junctions, and a resistance R_{m} (G_{m}) and a capacitance C_{m} that represent the total resistance and capacitance, respectively, of all the membranes of the coupled cells. These aggregate values are related to respective values for single cells in the following manner:

$$C_{\mathrm{m}} = nC_{\mathrm{m1}}, \quad R_{\mathrm{m}} = R_{\mathrm{m1}}/n \quad \text{and} \quad R_{\mathrm{j,tot}} = R_{\mathrm{j}}/n. \tag{3.3}$$

Hence,

$$G_{\mathrm{j,tot}} = nG_{\mathrm{j}} \quad \text{and} \quad G_{\mathrm{m}} = nG_{\mathrm{m1}}. \tag{3.4}$$

The time constant τ for charging the capacitance C_{m} in this circuit is equal to

$$\tau = \frac{R_{\mathrm{m}} R_{\mathrm{j,tot}} C_{\mathrm{m}}}{R_{\mathrm{m}} + R_{\mathrm{j,tot}}} = \frac{C_{\mathrm{m}}}{G_{\mathrm{j,tot}} + G_{\mathrm{m}}} = \frac{C_{\mathrm{m1}}}{G_{\mathrm{j}} + G_{\mathrm{m1}}}. \tag{3.5}$$

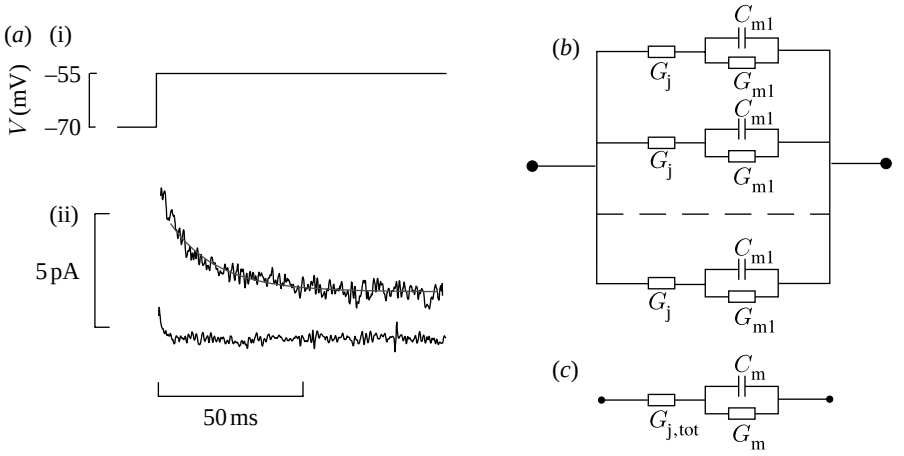

Figure 3. Capacitive currents during subthreshold depolarization in islet cells. (*a*(i)) A 15 mV depolarizing pulse was applied for 100 ms from a holding potential of −70 mV. (ii) The resultant current responses in a β-cell (*upper*) and a non-β-cell (*lower*) in an intact islet. The current responses represent the average of four individual sweeps. (*b*) Equivalent circuit for the β-cell. (*c*) Simplified equivalent circuit.

The derivation of this relationship takes into account that the resistances R_m and $R_{j,tot}$ are *not* coupled in series since a response of the circuit to alternating currents is being considered. Note that this is in contrast to our earlier analysis (equation (3.2)) where we consider direct currents. Details of the derivation are given in appendix A. From the observed value of τ, the value of G_j can be determined using these relationships. The value of G_j is dependent on the electrical characteristics of the individual coupled cell. This is because all coupled cells are connected in parallel. Again, we assume that the effects of cells attached to closest neighbours are small and can be neglected in this context (Goforth *et al.* 2002). Simple rearrangement of the equation (3.5) yields

$$G_j = \frac{C_{m1} - \tau G_{m1}}{\tau}. \tag{3.6}$$

Inserting numerical values ($C_{m1}=7.4$ pF, $G_{m1}=2.7$ GΩ and $\tau=13.5$ ms) into this equation gives an estimate of G_j of 0.18 nS. The latter value is in good agreement with the 0.17 nS derived for G_j based on the analysis of the action currents (figure 2*c*).

We also estimated the electrical charge Q (integrated current) that is needed to charge the membranes of all cells directly coupled to the patched cell. This charge was found by integrating the slow capacitive current ($Q=\int I(t)\mathrm{d}t$, where $I(t)$ is the time-dependent capacitive current) from figure 3*a*. In a series of five experiments carried out on functionally identified β-cells, the charge thus estimated averaged to 217 ± 46 fC. The relationship between charge Q, membrane capacitance C_{m1} and voltage change across it ΔV is given by the expression $Q=C_{m1}\cdot\Delta V$. Given that a neighbouring coupled cell experiences approximately 30 per cent of the voltage applied to the voltage-clamped cells (i.e. 27 mV out of the 86 mV applied to patched cell; see above), then the membrane potential of the electrically coupled cell will change by approximately

5 mV during the 15 mV voltage pulse. This assumption is valid because the electric elements involved are linear and do not depend on voltage. In a cell with a membrane capacitance of 7.4 pF, this voltage change requires a charge transfer of 34 fC. Comparing this value with the 217 fC obtained by the integration of the current response indicates that every β-cell is electrically connected with another six to seven β-cells.

(*e*) *Absence of dye coupling between β-cells*

Lucifer yellow has previously been used to visualize coupling between islet cells (Meda *et al.* 1986; Charollais *et al.* 2000). Patch electrodes were filled with Lucifer yellow (2 μM) and the cell was imaged on a confocal microscope. A set of images from a representative experiment is shown in figure 4*a*. Lucifer yellow accumulates within the nucleus (see arrows), providing a means of establishing the number of cells labelled. In a series of 10 experiments, no sign of dye coupling was observed and only the cells connected to the patch electrodes were stained. Despite the lack of dye coupling, the cells were clearly electrically coupled as evidenced by the occurrence of inverted action potentials during whole-cell voltage-clamp recordings (figure 4*b*). The absence of detectable dye coupling in electrically coupled β-cells is in agreement with recent reports from another laboratory (Quesada *et al.* 2003).

In many cells (including the one shown in figure 4*b*), the oscillations in holding current reflecting action potential firing in neighbours fluctuated between different levels. An unusually clear example of three discrete current levels present is seen in figure 4*c*. The amplitude of these steps was approximately 5 pA in this cell. We attribute these steps to the unsynchronized initiation of action potentials in increasing the number of neighbouring cells. Thus, it appears that the cell in figure 3*c* was electrically connected to at least three neighbours.

(*f*) *Effects of cell coupling on measurements of K_{ATP} conductance*

The gap junctional coupling of β-cells in intact mouse pancreatic islets is too weak to affect measurements of the voltage-gated currents over the physiological voltage range (cf. figure 1*b*). By contrast, cell coupling will affect recordings of currents that are not voltage gated. These include the K_{ATP} conductance, which represents the glucose-regulated membrane conductance in the β-cell (Ashcroft & Rorsman 1989). The resting conductance of the cell membrane is traditionally monitored by applying 10–20 mV pulses from a holding potential at −70 mV. In β-cells within intact islets, the resting conductance in the patch-clamped cell is the sum of the gap junctional conductance (G_j), unknown leak conductance (G_{leak}) and the whole-cell K_{ATP} conductance ($G_{K,ATP}$). For mouse islets, the total resting conductance varies between 3.6 nS in the absence of glucose and 1.1 nS in the presence of glucose concentrations of 20 mM glucose and above or following the addition of the K_{ATP} channel blocker tolbutamide (Göpel *et al.* 1999*a*). Given that the method used to obtain the data presented in figure 1 measures the gap junctional conductance only and does *not* detect any leak conductance, it may seem surprising that the resting conductance measured at 20 mM glucose (that will be contaminated by leak currents) is lower (1.1 nS) than the coupling conductance obtained by the evaluation of the coupling currents

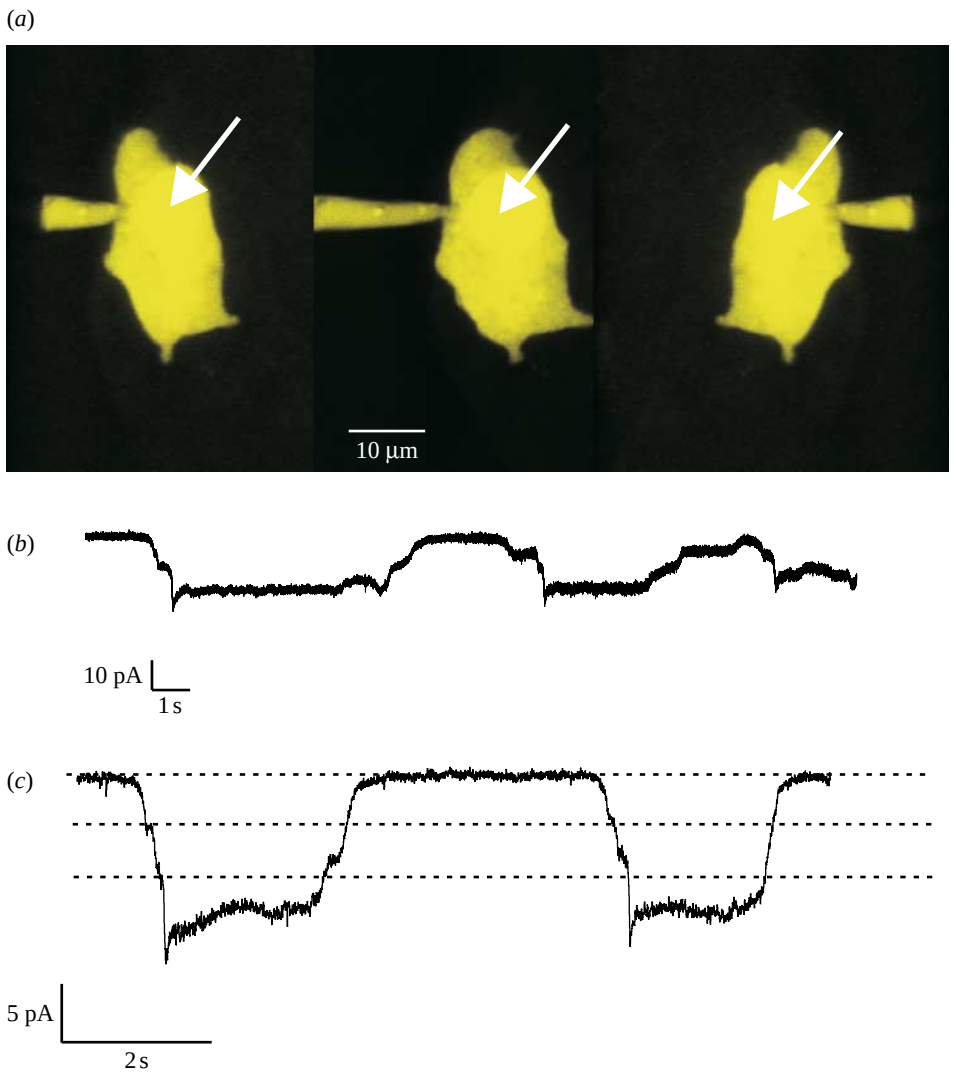

Figure 4. No evidence of dye coupling between β-cells. (*a*) Confocal image of a β-cell in an intact islet which had been dialysed with Lucifer yellow (2 µM) via the recording electrode. Three different projections of the same cells are shown. Lucifer yellow accumulates in the nucleus (*arrows*). (*b*) Recording of membrane currents in the same cell as shown in (*a*) when the membrane was held at −70 mV. (*c*) Same type of recording from another β-cell showing clear stepwise increases in current. In (*b*,*c*), β-cell identity was established by the absence of detectable voltage-gated Na^+ currents when holding at −70 mV (Göpel *et al.* 1999*a*).

in figure 1 (1.22 nS). However, there is a simple and functionally significant explanation of this finding.

Consider the equivalent circuit shown in figure 5*a*. This circuit represents the network of three main conductances $G_{K,ATP}$, G_{leak} and G_j for two coupled cells. It can be seen that the gap junctional conductance is in series with all other membrane conductances in the cell coupled to the patch-clamped cell (forthwith referred to as

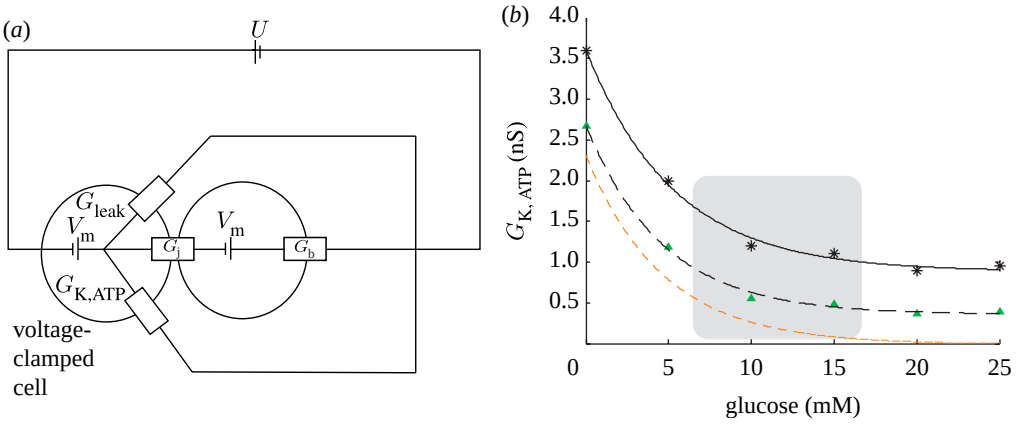

Figure 5. Influence of gap junctional conductance on resting glucose-regulated membrane conductance. (*a*) Equivalent circuit for two coupled cells including K_{ATP} ($G_{K,ATP}$), leak (G_{leak}) and gap junctional conductances (G_j). The gap junctions in the voltage-clamped cell are in series with all membrane conductances of the coupled cells but in parallel with its plasmalemmal ionic conductances (including $G_{K,ATP}$ and G_{leak}). (*b*) Resting β-cell conductance measured in intact islets at different glucose concentrations (asterisks and solid curve). Data points are taken from Göpel *et al.* (1999*a*). The green triangles and dashed curve represent the background current that consists of G_{leak} and $G_{K,ATP}$ in coupled cells calculated according to equation (3.10) (see main text). The red curve represents the net $G_{K,ATP}$ in the patch-clamped cell after correction for the variable contribution of the background current, which is dependent on the junctional conductance. The grey shaded area highlights glucose-dependent changes of $G_{K,ATP}$ between 7 and 17 mM glucose.

the 'background conductance' G_b). The whole-cell resting conductance (G_R) is then given by the expression

$$G_R = G_{K,ATP} + G_{leak} + \left(\frac{1}{G_j} + \frac{1}{G_b}\right)^{-1}. \tag{3.7}$$

In the absence of glucose (i.e when $G_{K,ATP}$ is high), most of the voltage drop will occur across the gap junctions since this resistance is higher than that of the cell membrane coupled in series to the gap junction (5.9 versus 2.7 GΩ). Glucose-induced closure of the K_{ATP} channels reduces the resting conductance not only by the closure of the channels located in the patch-clamped cell but also in the neighbouring cells, thus leading to a reduction of G_b. Consequently, measurements of $G_{K,ATP}$ are influenced by cell coupling. When $G_{K,ATP}$ is high, coupling contributes only marginally to the measured G_R. This is because G_j is low compared with $G_{K,ATP}$ and most of the current passing through the recording electrode will leave via the K_{ATP} channels. As glucose is elevated and $G_{K,ATP}$ falls, an increasing proportion of the current will pass via G_j and eventually (when $G_{K,ATP}=0$) G_j will become dominant because it consists of several membrane and leak conductances connected in parallel. Accordingly, the contribution of cell coupling to the measured G_R will vary at different glucose concentrations.

Figure 5*b* shows the glucose dependence of the β-cell resting K_{ATP} conductance after correction for the variable G_b. The correction was calculated for six coupled

identical cells as follows. First, we rewrite, for n coupled cells, the equation for the resting conductance G_R taking into account additionally that the background conductance $G_b = G_{K,ATP} + G_{leak}$. This gives the following equation:

$$G_R = G_b + n\frac{G_j G_b}{G_j + G_b}. \tag{3.8}$$

Solving this for G_b (dashed curve in figure 5*b*) results in the expression

$$G_b = \sqrt{\frac{[(n+1)G_j - G_R]^2}{4} + G_R \cdot G_j} - \frac{(n+1)G_j - G_R}{2}. \tag{3.9}$$

At high glucose concentrations, when $G_{K,ATP}$ approaches zero, G_b becomes equal to G_{leak}. The corrected curve for $G_{K,ATP}$ (red dashed curve in figure 5*b*) can then be obtained by subtracting G_b at 25 mM glucose (forthwith referred to as G_{25G}) from G_b, i.e.

$$G_{K,ATP,corrected} = G_b - G_{25G}. \tag{3.10}$$

The net $G_{K,ATP}$ (red dashed curve) falls from 2.3 nS at 0 mM glucose to zero at glucose concentrations above 20 mM glucose with an IC_{50} of 3.7 mM.

(*g*) *Propagation of* $[Ca^{2+}]_i$ *waves in an islet*

$[Ca^{2+}]_i$ imaging experiments have revealed that the $[Ca^{2+}]_i$ oscillations in different parts of an islet are well synchronized (Valdeolmillos *et al.* 1989; Santos *et al.* 1991). Can the widespread Ca^{2+} oscillations be accounted for by the electrical coupling we measure here? To address this question, we performed $[Ca^{2+}]_i$ imaging in intact mouse islets in the absence and presence of 20 mM glucose. As shown in figure 6*a*, addition of 20 mM glucose (after an initial lowering of $[Ca^{2+}]_i$) triggers oscillations in $[Ca^{2+}]_i$ in individual β-cells (three examples shown) that were not active in the absence of sugar. These oscillations are sufficiently well coupled to result in synchronized $[Ca^{2+}]_i$ oscillations that can be resolved at the whole-islet level.

In addition to the $[Ca^{2+}]_i$ oscillations evoked by high glucose, a subset of cells were active in the absence of glucose. These cells are likely to be glucagon-producing α-cells (figure 6*b*). The $[Ca^{2+}]_i$ oscillations in these cells were not synchronized and therefore could not be resolved at the whole-islet level (figure 6*a*,*b*; grey shaded areas).

We analysed the spread of the $[Ca^{2+}]_i$ wave in intact mouse islets. Figure 6*c* shows an example where the propagation of a $[Ca^{2+}]_i$ wave was monitored along the periphery of the islet in eight different cells. The penetration of the Ca^{2+} indicator into deeper cell layers was insufficient to allow accurate $[Ca^{2+}]_i$ imaging in the islet centre. The wave started in cell 1 and then travelled with a speed ranging between 8 μm s^{-1} (between cells 3 and 4) and above 149 μm s^{-1} (between cells 2 and 3 and cells 6 and 7) with an average of 57 μm s^{-1}. In a series of four experiments/islets conducted in the presence of 20 mM glucose and analysed similarly, the $[Ca^{2+}]_i$ wave propagated at an average velocity of 81 ± 11 μm s^{-1}.

(*h*) *Is electrical coupling sufficient to account for islet* $[Ca^{2+}]_i$ *synchronization?*

We examined whether electrical coupling between β-cells is sufficient to synchronize β-cells across the islets. Consider the time required to charge the

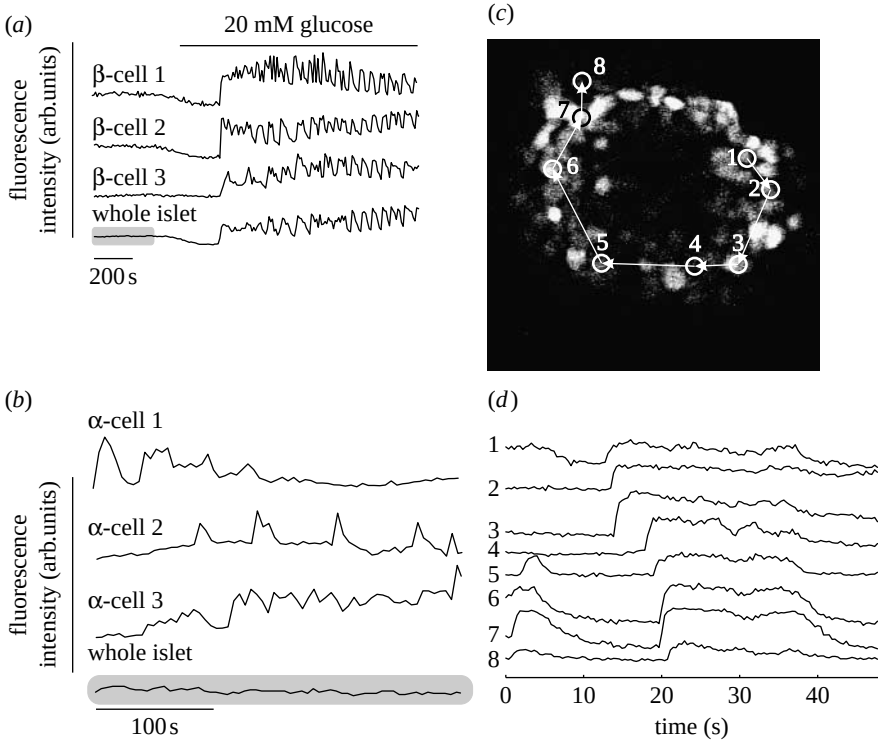

Figure 6. Propagation of $[Ca^{2+}]_i$ waves in intact mouse islets. (*a*,*b*) Recordings of $[Ca^{2+}]_i$ at 1 and 20 mM glucose from (*a*) three different β-cells and (*b*) three different α-cells. The whole-islet responses are also shown. The period highlighted in (*b*) is the same as that highlighted in (*a*) (note the use of different time scales). Whereas the $[Ca^{2+}]_i$ oscillations in the β-cells are sufficiently synchronized to be observable at the whole-islet level, this is not the case for the α-cells. (*c*) Confocal image of a mouse islet loaded with fluo-4. The positions of eight different cells are shown. The $[Ca^{2+}]_i$ wave propagated as indicated by the arrows. (*d*) $[Ca^{2+}]_i$ oscillations recorded from the eight cells indicated in (*c*). Note that there is a progressive delay in the responses and that the wave appears to move along the islet periphery clockwise.

membrane capacitance of a β-cell by current injection. For these calculations, the β-cell is represented by an equivalent circuit composed of a resistance R connected in parallel with a capacitance C. If current i_{inj} is applied to the input of this circuit, then, according to Kirchhoff's laws, the time dependence of the amount of charge q on C is described by a differential equation,

$$\frac{\mathrm{d}q}{\mathrm{d}t} + \frac{1}{RC}q = i_{\mathrm{inj}}. \tag{3.11}$$

A partial solution of this differential equation with an initial condition $q{=}0$ when $t{=}0$ is

$$\Delta V = \frac{q}{C} = i_{\mathrm{inj}}R(1 - \mathrm{e}^{-t/RC}). \tag{3.12}$$

Here ΔV is the change of voltage across the cell membrane at time t. Solving equation (3.12) for t yields an expression that allows us to calculate the charging

time of the cell,

$$t = -RC \ln\left(1 - \frac{\Delta V}{i_{\mathrm{inj}} R}\right). \tag{3.13}$$

In five cells with clear bursting pattern of electrical activity, the amplitude of the burst (from the most hyperpolarized voltage to the peak of the action potential) averaged -42 ± 2 mV. In the same experiments, the 'pacemaker' depolarization (ΔV; see figure 2*a* for definition) between two successive bursts averaged 5 ± 2 mV. With these values of ΔV and taking R, C and the gap junctional conductance to be 2.7 GΩ, 7.4 pF and 0.17 nS, respectively, equation (3.13) can be simplified to

$$t = -20.0 \times 10^{-3} \ln(1 - 2/i_{\mathrm{inj}}). \tag{3.14}$$

The expression reveals that the minimum value of i_{inj} that will be capable of charging the cell is 2 pA. With a burst amplitude of 42 mV, i_{inj} can be estimated to be 7.1 pA. Inserting this value into equation (3.14), the time needed to charge a neighbour is approximately 7 ms.

4. Discussion

It is well established that electrical activity within a mouse pancreatic islet is synchronized (Meissner 1976; Eddlestone *et al.* 1984; Mears *et al.* 1995) and results in coordinated oscillations in $[Ca^{2+}]_i$ across the islet (Valdeolmillos *et al.* 1989; Santos *et al.* 1991). Cell coupling has been proposed to explain the synchronization of β-cell electrical activity (Meda *et al.* 1986; Charollais *et al.* 2000), but it is also possible that signalling by autocrine and paracrine factors is involved (Salehi *et al.* 2005).

A detailed characterization of the membrane currents in islet cells requires the means of voltage clamping these cells. We have developed techniques that allow patch-clamp recordings from cells in intact islets (Göpel *et al.* 1999*a*). It is possible that cell coupling can interfere with these measurements and that regenerative processes in neighbouring cells (that are not voltage clamped) might contaminate the signals measured in the cell in direct contact with the recording electrode. Here, we have analysed the extent of cell coupling in intact mouse pancreatic islets combining voltage-clamp and current-clamp measurements with confocal $[Ca^{2+}]_i$ imaging. The fact that some measurements were conducted under voltage-clamp conditions (when the membrane potential is controlled) enables us to distinguish between whole-cell conductances that are attributable to cell coupling and those that arise from the activity of ion channels. We show that whereas cell coupling does not interfere with the measurements of voltage-gated currents, it contributes to the measured resting conductance. Theoretical considerations further suggest that although cell coupling in the islet is fairly weak, it is of sufficient strength to explain the synchronization of electrical activity and $[Ca^{2+}]_i$ in the islet that underlie pulsatile insulin secretion (Gilon *et al.* 1993).

(*a*) *Pancreatic β-cells are weakly coupled to each other*

The *total* gap junctional conductance between a β-cell and its neighbours amounts to approximately 1.22 nS (0.8 GΩ). By analogy to a similar patch-clamp study on the cell coupling between chromaffin cells within adrenal slices (Moser

1998), we conclude that the gap junctional conductance between β-cells *in situ* is too low to allow voltage clamping of the neighbouring cells. We estimate that only approximately 30 per cent of the voltage change imposed on the voltage-clamped cell spreads into the neighbours (see figure 2). This means that during depolarizations from −70 mV to voltages below 0 mV, the membrane potential in the electrically coupled neighbours will not exceed the threshold for firing an action potential and the observed current responses will principally (if not exclusively) reflect the ionic currents flowing through the membrane of the voltage-clamped cell. During larger voltage steps, however, the threshold will eventually be exceeded and the resultant action potential(s) in the unclamped neighbours will give rise to large transients superimposed on the current responses. However, it takes a fairly long time for these current transients to appear even during strong depolarizations and the current amplitude can be determined accurately during the first approximately 10 ms after the application of the depolarizing pulse. Reassuringly, the voltage dependence of the voltage-gated membrane currents measured in β-cells in intact islets is the same as in isolated cells (Rorsman & Trube 1986; Göpel *et al.* 1999*a*).

Based on the analysis of the firing of action potentials and the slow capacitive currents elicited by subthreshold stimuli, we estimate that every β-cell is coupled to approximately seven other β-cells. Interestingly, dye-coupling experiments have indicated a similar value for the number of coupled cells (Charollais *et al.* 2000). Our value for the gap junctional conductance between *two* β-cells within the islet is 0.17–0.18 nS. This is in reasonable agreement with previous estimates obtained in isolated pairs of β-cells: 0.15 nS (Andreu *et al.* 1997) and 0.22 nS (Perez-Armendariz *et al.* 1991).

(*b*) *Effects of coupling on measurements of the K_{ATP} conductance*

Because the gap junctions of the cells in direct contact with the patch-clamped cell in electrical terms are connected in parallel, cell coupling will *not* affect the voltage clamp of the cell connected to the pipette and properties of the voltage-gated currents can thus be expected to be reported accurately. However, cell coupling will affect measurements of the resting conductance. Thus, the relationships between K_{ATP} whole-cell conductance ($G_{K,ATP}$) and the glucose concentration that have been reported previously (figure 5 and Göpel *et al.* 1999*a*) must be corrected for the contribution of cell coupling. The original data indicated a drop in conductance from approximately 4 nS to approximately 1 nS when the glucose concentration is increased from 0 to 20 mM (figure 5*b*). After correction for coupling, $G_{K,ATP}$ instead falls from a maximum value of 2.3 nS in the absence of glucose to values close to or less than 0.1 nS at glucose concentrations exceeding 15 mM (figure 5). Importantly, an increase in glucose from 7 to 17 mM is associated with a reduction of the corrected $G_{K,ATP}$ from 0.61 nS to 0.07 nS (figure 5*b*, grey shaded area). Thus, glucose influences $G_{K,ATP}$ over a wide range of glucose concentrations in a way that may contribute to the concentration-dependent increase in β-cell electrical activity observed at intermediate glucose concentrations (Henquin & Meissner 1984; Kanno *et al.* 2002). It also accounts for the ability of the sulphonylureas to convert oscillatory electrical activity into continuous action potential firing.

(c) Non-β-cells are not electrically coupled

In addition to confirming the existence of coupling between β-cells, this study extends previous observations indicating lack of coupling between non-β-cells (Göpel *et al.* 1999*a*). Thus, no slow capacitive current was observed in response to subthreshold depolarizations in non-β-cells (identified by the presence of a Na^+ current that can be activated from a holding potential of 70 mV). We acknowledge that our failure to detect any evidence for electrical coupling between non-β-cells is at variance with earlier electrophysiological (Meda *et al.* 1986), dye-coupling (Michaels & Sheridan 1981) and ultrastructural studies (Orci *et al.* 1975). However, recent experiments employing confocal imaging of the cytoplasmic Ca^{2+} concentration have revealed that Ca^{2+} in both glucagon-secreting α-cells and somatostatin-producing δ-cells, unlike the β-cells, oscillates asynchronously (Nadal *et al.* 1999; Quesada *et al.* 1999) and our data support these observations (figure 6*b*). Given that both α- and δ-cells have a high input resistance (Bokvist *et al.* 1999; Barg *et al.* 2000; Göpel *et al.* 2000*a*,*b*), it appears that coupling between β- and non-β-cells must be weak as even the small currents entering via the gap junctions would otherwise have dramatic effects on the membrane potential of these cells. Thus, we propose that weak coupling is a prerequisite to allow electrical activity and secretion to be differentially (β- and δ-cells; Zhang *et al.* 2007) and reciprocally (β- and δ-cells versus α-cells; Macdonald *et al.* 2007) regulated by glucose.

(d) Cell coupling is sufficient to account for propagation of $[Ca^{2+}]_i$ waves

Mouse β-cells exposed to insulin-releasing glucose concentration exhibit $[Ca^{2+}]_i$ oscillations that can be resolved at both the single-cell and the whole-islet level. It is possible that these oscillations are due to electrical coupling, but it has also been proposed that diffusible factors co-released with insulin (such as ATP) underlie synchronization (Salehi *et al.* 2005).

The time to charge a neighbour via the gap junctions is as short as 7 ms. Yet, we observe a delay of several seconds between the onset of a $[Ca^{2+}]_i$ wave in different parts of the islet (figure 6). However, the passive electrical spread of impulses across the islet only accounts for a small part of the delay, which is mainly (95%) attributable to the time it takes to initiate an action potential after the depolarization of the cell membrane. In our experiments, this parameter averaged approximately 165 ms, and we thus arrive at a total value of 172 ms for the propagation of an action potential from one cell to another. With a cell diameter of approximately 15 μm, we estimate that the $[Ca^{2+}]_i$ wave will travel with a speed of 88 $\mu m\, s^{-1}$ (15 μm/0.17 s). This is in surprisingly good agreement with the 81 $\mu m\ s^{-1}$ observed in the confocal $[Ca^{2+}]_i$ imaging experiments (figure 6*c*,*d*).

Can cell coupling be of pathophysiological significance? It was recently reported that in mice expressing non-functional K_{ATP} channels in 70 per cent of the β-cells, normal K_{ATP} channel activity in the remaining cells, the communication between normal and impaired cells, via cell coupling, is sufficient to restore nearly normal glucose regulation of $[Ca^{2+}]_i$ and insulin secretion (Rocheleau *et al.* 2006). Conversely, an increase in K_{ATP} channel, due to an impairment of metabolism in a minority of β-cells, will via the reduction in input resistance impede the passive spread of depolarization across the islet (see equation (3.12)). Thus, small changes in either the gap junctional conductance and/or the amplitude of the bursts may

have dramatic effects on cell coupling, the synchronization of the $[Ca^{2+}]_i$ waves and thus the pulsatility of insulin secretion. Given that type-2 diabetes is associated with the loss of pulsatile insulin secretion in both rodents (Lin *et al.* 2001) and humans (Lang *et al.* 1981), it should therefore be considered whether this defect is attributable to impaired electrical coupling between the β-cells.

This work was supported by the Wellcome Trust, the Swedish Research Council (L.E.) and the European Union through BioSim (contract no. LSHB-CT-2004-005137) and Eurodia (contract no. LSHM-CT-2006-518153). F.A. is on leave from the University of São Paulo, Brazil, on a CNPq fellowship—Conselho Nacional de Desenvolvimento Científico e Tecnológico, Brazil. L.E. is employed by the Lund University Diabetes Centre and P.R. is a Wolfson-Royal Society Merit Award Fellow.

Appendix A

The current in the circuit shown in figure 3*c* reaches a constant value after an application of a voltage step in time τ, which is determined by the elements comprising the circuit. A straightforward application of Kirchhoff's laws shows that the relaxation process in this circuit is described by a differential equation,

$$\frac{\mathrm{d}U}{\mathrm{d}t} + \frac{R_1 + R_2}{CR_1R_2}\,U - \frac{U_0}{CR_1} = 0. \tag{A 1}$$

The solution of this equation at initial condition $U(0)=0$ is

$$U = \frac{U_0 R_2}{R_1 + R_2}\left(1 - \exp\left(-\frac{R_1 + R_2}{CR_1R_2}\,t\right)\right). \tag{A 2}$$

Here U and t are voltage and time, respectively. It follows from equation (A 2) that the relaxation time constant τ in this circuit is $\tau = CR_1R_2/(R_1+R_2)$.

References

Andreu, E., Soria, B. & Sanchez-Andres, J. V. 1997 Oscillation of gap junction electrical coupling in the mouse pancreatic islets of Langerhans. *J. Physiol.* **498**(Pt. 3), 753–761.

Ashcroft, F. M. & Rorsman, P. 1989 Electrophysiology of the pancreatic β-cell. *Prog. Biophys. Mol. Biol.* **54**, 87–143. (doi:10.1016/0079-6107(89)90013-8)

Atwater, I., Ribalet, B. & Rojas, E. 1979 Mouse pancreatic beta-cells: tetraethylammonium blockage of the potassium permeability increase induced by depolarization. *J. Physiol.* **288**, 561–574.

Barg, S., Galvanovskis, J., Göpel, S. O., Rorsman, P. & Eliasson, L. 2000 Tight coupling between electrical activity and exocytosis in mouse glucagon-secreting alpha-cells. *Diabetes* **49**, 1500–1510. (doi:10.2337/diabetes.49.9.1500)

Bokvist, K., Olsen, H. L., Høy, M., Gotfredsen, C. F., Holmes, W. F., Buschard, K., Rorsman, P. & Gromada, J. 1999 Characterisation of sulphonylurea and ATP-regulated K^+ channels in rat pancreatic A-cells. *Pflugers Arch.* **438**, 428–436. (doi:10.1007/s004240051058)

Calabrese, A., Zhang, M., Serre-Beinier, V., Caton, D., Mas, C., Satin, L. S. & Meda, P. 2003 Connexin 36 controls synchronization of Ca^{2+} oscillations and insulin secretion in MIN6 cells. *Diabetes* **52**, 417–424. (doi:10.2337/diabetes.52.2.417)

Charollais, A. *et al.* 2000 Junctional communication of pancreatic β cells contributes to the control of insulin secretion and glucose tolerance. *J. Clin. Invest.* **106**, 235–243. (doi:10.1172/JCI9398)

Eddlestone, G. T., Goncalves, A., Bangham, J. A. & Rojas, E. 1984 Electrical coupling between cells in islets of Langerhans from mouse. *J. Memb. Biol.* **77**, 1–14. (doi:10.1007/BF01871095)

Gilon, P., Shepherd, R. M. & Henquin, J. C. 1993 Oscillations of secretion driven by oscillations of cytoplasmic Ca^{2+} as evidences in single pancreatic islets. *J. Biol. Chem.* **268**, 22 265–22 268.

Goforth, P. B., Bertram, R., Khan, F. A., Zhang, M., Sherman, A. & Satin, L. S. 2002 Calcium-activated K^+ channels of mouse β-cells are controlled by both store and cytoplasmic Ca^{2+}: experimental and theoretical studies. *J. Gen. Physiol.* **120**, 307–322. (doi:10.1085/jgp.20028581)

Göpel, S., Kanno, T., Barg, S., Galvanovskis, J. & Rorsman, P. 1999*a* Voltage-gated and resting membrane currents recorded from B-cells in intact mouse pancreatic islets. *J. Physiol.* **521**(Pt. 3), 717–728. (doi:10.1111/j.1469-7793.1999.00717.x)

Göpel, S. O., Kanno, T., Barg, S., Eliasson, L., Galvanovskis, J., Renström, E. & Rorsman, P. 1999*b* Activation of Ca^{2+}-dependent K^+ channels contributes to rhythmic firing of action potentials in mouse pancreatic β cells. *J. Gen. Physiol.* **114**, 759–770. (doi:10.1085/jgp.114.6.759)

Göpel, S. O., Kanno, T., Barg, S. & Rorsman, P. 2000*a* Patch-clamp characterisation of somatostatin-secreting δ-cells in intact mouse pancreatic islets. *J. Physiol.* **528**(Pt. 3), 497–507. (doi:10.1111/j.1469-7793.2000.00497.x)

Göpel, S. O., Kanno, T., Barg, S., Weng, X. G., Gromada, J. & Rorsman, P. 2000*b* Regulation of glucagon release in mouse-cells by K_{ATP} channels and inactivation of TTX-sensitive Na^+ channels. *J. Physiol.* **528**(Pt. 3), 509–520. (doi:10.1111/j.1469-7793.2000.00509.x)

Henquin, J. C. & Meissner, H. P. 1984 Significance of ionic fluxes and changes in membrane potential for stimulus–secretion coupling in pancreatic B-cells. *Experientia* **40**, 1043–1052. (doi:10.1007/BF01971450)

Hille, B. 2001 *Ion channels of excitable membranes*. Sunderland, MA: Sinauer.

Kanno, T., Rorsman, P. & Göpel, S. O. 2002 Glucose-dependent regulation of rhythmic action potential firing in pancreatic β-cells by K_{ATP}-channel modulation. *J. Physiol.* **545**, 501–507. (doi:10.1113/jphysiol.2002.031344)

Lang, D. A., Matthews, D. R., Burnett, M. & Turner, R. C. 1981 Brief, irregular oscillations of basal plasma insulin and glucose concentrations in diabetic man. *Diabetes* **30**, 435–439. (doi:10.2337/diabetes.30.5.435)

Lin, J.-M., Ortsäter, H., Fakhrai-Rad, H., Galli, J., Luthman, H. & Bergsten, P. 2001 Phenotyping of individual pancreatic islets locates genetic defects in stimulus secretion coupling to *Niddm1i* within the major diabetes locus in GK rats. *Diabetes* **50**, 2737–2743. (doi:10.2337/diabetes.50.12.2737)

Luther, M. J., Hauge-Evans, A., Souza, K. L., Jorns, A., Lenzen, S., Persaud, S. J. & Jones, P. M. 2006 MIN6 β-cell–β-cell interactions influence insulin secretory responses to nutrients and non-nutrients. *Biochem. Biophys. Res. Commun.* **343**, 99–104. (doi:10.1016/j.bbrc.2006.02.003)

Macdonald, P. E., Marinis, Y. Z., Ramracheya, R., Salehi, A., Ma, X., Johnson, P. R., Cox, R., Eliasson, L. & Rorsman, P. 2007 A K_{ATP} channel-dependent pathway within α cells regulates glucagon release from both rodent and human islets of Langerhans. *PLoS Biol.* **5**, e143. (doi:10.1371/journal.pbio.0050143)

Mears, D., Sheppard Jr, N. F., Atwater, I. & Rojas, E. 1995 Magnitude and modulation of pancreatic β-cell gap junction electrical conductance *in situ*. *J. Memb. Biol.* **146**, 163–176. (doi:10.1007/BF00238006)

Meda, P., Santos, R. M. & Atwater, I. 1986 Direct identification of electrophysiologically monitored cells within intact mouse islets of Langerhans. *Diabetes* **35**, 232–236. (doi:10.2337/diabetes.35.2.232)

Meissner, H. P. 1976 Electrophysiological evidence for coupling between β-cells of pancreatic islets. *Nature* **262**, 502–504. (doi:10.1038/262502a0)

Michaels, R. L. & Sheridan, J. D. 1981 Islets of Langerhans: dye coupling among immunocytochemically distinct cell types. *Science* **214**, 801–803. (doi:10.1126/science.6117129)

Moser, T. 1998 Low-conductance intercellular coupling between mouse chromaffin cells *in situ*. *J. Physiol.* **506**(Pt. 1), 195–205. (doi:10.1111/j.1469-7793.1998.195bx.x)

Nadal, A., Quesada, I. & Soria, B. 1999 Homologous and heterologous asynchronicity between identified α-, β- and δ-cells within intact islets of Langerhans in the mouse. *J. Physiol.* **517**(Pt. 1), 85–93. (doi:10.1111/j.1469-7793.1999.0085z.x)

Orci, L., Malaisse-Lagae, F., Amherdt, M., Ravazzola, M., Weisswange, A., Dobbs, R., Perrelet, A. & Unger, R. 1975 Cell contacts in human islets of Langerhans. *J. Clin. Endocrinol. Metab.* **41**, 841–844.

Perez-Armendariz, M., Roy, C., Spray, D. C. & Bennett, M. V. 1991 Biophysical properties of gap junctions between freshly dispersed pairs of mouse pancreatic beta cells. *Biophys. J.* **59**, 76–92.

Pipeleers, D. 1987 The biosociology of pancreatic B cells. *Diabetologia* **30**, 277–291. (doi:10.1007/BF00299019)

Pipeleers, D., in't Veld, P. I., Maes, E. & Van De Winkel, M. 1982 Glucose-induced insulin release depends on functional cooperation between islet cells. *Proc. Natl Acad. Sci. USA* **79**, 7322–7325. (doi:10.1073/pnas.79.23.7322)

Quesada, I., Fuentes, E., Andreu, E., Meda, P., Nadal, A. & Soria, B. 2003 On-line analysis of gap junctions reveals more efficient electrical than dye coupling between islet cells. *Am. J. Physiol. Endocrinol. Metab.* **284**, E980–E987.

Quesada, I., Nadal, A. & Soria, B. 1999 Different effects of tolbutamide and diazoxide in alpha, beta-, and delta-cells within intact islets of Langerhans. *Diabetes* **48**, 2390–2397. (doi:10.2337/diabetes.48.12.2390)

Renström, E., Eliasson, L., Bokvist, K. & Rorsman, P. 1996 Cooling inhibits exocytosis in single mouse pancreatic B-cells by suppression of granule mobilization. *J. Physiol.* **494**(Pt. 1), 41–52.

Rocheleau, J. V., Remedi, M. S., Granada, B., Head, W. S., Koster, J. C., Nichols, C. G. & Piston, D. W. 2006 Critical role of gap junction coupled K_{ATP} channel activity for regulated insulin secretion. *PLoS Biol.* **4**, e26. (doi:10.1371/journal.pbio.0040026)

Rorsman, P., Berggren, P. O., Bokvist, K., Ericson, H., Mohler, H., Ostenson, C. G. & Smith, P. A. 1989 Glucose-inhibition of glucagon secretion involves activation of GABAA-receptor chloride channels. *Nature* **341**, 233–236. (doi:10.1038/341233a0)

Rorsman, P. & Renström, E. 2003 Insulin granule dynamics in pancreatic beta cells. *Diabetologia* **46**, 1029–1045. (doi:10.1007/s00125-003-1153-1)

Rorsman, P. & Trube, G. 1986 Calcium and delayed potassium currents in mouse pancreatic beta-cells under voltage-clamp conditions. *J. Physiol.* **374**, 531–550.

Salehi, A., Qader, S. S., Grapengiesser, E. & Hellman, B. 2005 Inhibition of purinoceptors amplifies glucose-stimulated insulin release with removal of its pulsatility. *Diabetes* **54**, 2126–2131. (doi:10.2337/diabetes.54.7.2126)

Santos, R. M., Rosario, L. M., Nadal, A., Garcia-Sancho, J., Soria, B. & Valdeolmillos, M. 1991 Widespread synchronous $[Ca^{2+}]_i$ oscillations due to bursting electrical activity in single pancreatic islets. *Pflugers Arch.* **418**, 417–422. (doi:10.1007/BF00550880)

Sheppard, M. S. & Meda, P. 1981 Tetraethylammonium modifies gap junctions between pancreatic beta-cells. *Am. J. Physiol.* **240**, C116–C120.

Valdeolmillos, M., Santos, R. M., Contreras, D., Soria, B. & Rosario, L. M. 1989 Glucose-induced oscillations of intracellular Ca^{2+} concentration resembling bursting electrical activity in single mouse islets of Langerhans. *FEBS Lett.* **259**, 19–23. (doi:10.1016/0014-5793(89)81484-X)

Willecke, K., Eiberger, J., Degen, J., Eckardt, D., Romualdi, A., Guldenagel, M., Deutsch, U. & Sohl, G. 2002 Structural and functional diversity of connexin genes in the mouse and human genome. *Biol. Chem.* **383**, 725–737. (doi:10.1515/BC.2002.076)

Zhang, Q. *et al.* 2007 R-type Ca^{2+}-channel-evoked CICR regulates glucose-induced somatostatin secretion. *Nat. Cell Biol.* **9**, 453–460. (doi:10.1038/ncb1563)